Accepted Manuscript

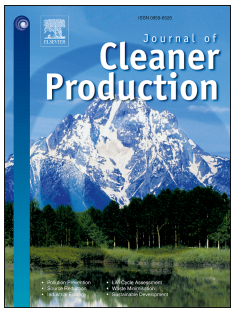

Bio-based synthesis of oxidation resistant copper nanowires using an aqueous plant extract

Ricardo J.B. Pinto, José M.F. Lucas, Fábio M. Silva, Ana V. Girão, Filipe J. Oliveira, Paula A.A.P. Marques, Carmen S.R. Freire

PII: S0959-6526(19)30588-8

DOI: https://doi.org/10.1016/j.jclepro.2019.02.189

Reference: JCLP 15919

To appear in: *Journal of Cleaner Production*

Received Date: 6 November 2018

Revised Date: 30 January 2019

Accepted Date: 17 February 2019

Please cite this article as: Pinto RJB, Lucas JoséMF, Silva FáM, Girão AV, Oliveira FJ, Marques PAAP, Freire CSR, Bio-based synthesis of oxidation resistant copper nanowires using an aqueous plant extract, *Journal of Cleaner Production* (2019), doi: https://doi.org/10.1016/j.jclepro.2019.02.189.

This is a PDF file of an unedited manuscript that has been accepted for publication. As a service to our customers we are providing this early version of the manuscript. The manuscript will undergo copyediting, typesetting, and review of the resulting proof before it is published in its final form. Please note that during the production process errors may be discovered which could affect the content, and all legal disclaimers that apply to the journal pertain.

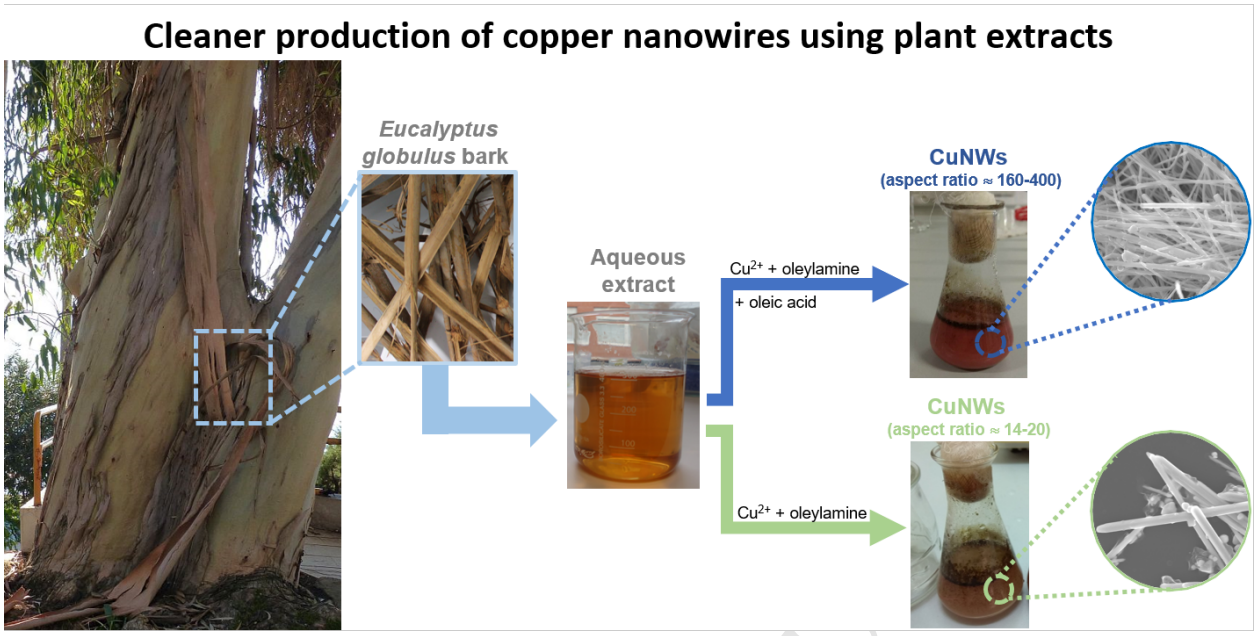

ACCEPTED MANUSCRIPT

ACCEPTED MANUSCRIPT

Document words: 7881

Bio-based synthesis of oxidation resistant copper nanowires using an aqueous plant extract

Ricardo J. B. Pinto,[a,c,*] *José M. F. Lucas,*[a] *Fábio M. Silva,*[a] *Ana V. Girão,*[b] *Filipe J. Oliveira,*[b] *Paula A. A. P. Marques,*[c] *Carmen S. R. Freire,*[a,*]

[a] Department of Chemistry-CICECO, University of Aveiro, 3810-193 Aveiro, Portugal

[b] Department of Materials and Ceramic Engineering - CICECO, University of Aveiro, 3810-193 Aveiro, Portugal

[c] TEMA – NRD, Mechanical Engineering Department and Aveiro Institute of Nanotechnology (AIN), University of Aveiro, 3810-193 Aveiro, Portugal

* E-mail: R.J.B. Pinto – r.pinto@ua.pt; C.S.R. Freire – cfreire@ua.pt.

ACCEPTED MANUSCRIPT

ABSTRACT

Copper nanowires have recently emerged as promising nanomaterials for transparent conducting electrodes applications, however, their production commonly involves the use of harmful reagents. In this study, we describe for the first time a simple and cost-effective bio-based synthesis of copper nanowires using an aqueous plant extract (*Eucalyptus globulus*) as the reducing/stabilizing agent and oleic acid and oleylamine as surfactants. Well-dispersed crystalline copper nanowires ($\lambda_{máx}$ = 584 to 613 nm) were obtained with average diameters in the nanometric range (44 and 145 nm) and lengths in the micrometric range (from 5 to dozens of micrometres) using extract concentrations between 10 and 50 $mg.ml^{-1}$. Moreover, the aspect ratio of these nanowires can be adjusted (from around 14-20 to 160-400) by changing the experimental conditions, namely the use of oleic acid. Phenolic compounds were found to have a key role in this bioreduction process allowing obtain practically only nanowires (without other morphologies). Nevertheless, the use of oleic acid/oleylamine is essential to manipulate the respective size and aspect ratio. Most importantly, these bio-based copper nanowires were found to be resistant under storage in ethanol and when submitted to air exposure, both for 2 weeks, certainly due to the adsorption of antioxidant biomolecules (phenolic) at their surface, thus avoiding the use of other polymeric protective layers. The conductivity of the CuNWs was found to be 0.009 $S.cm^{-1}$. As a result, this study opens a new standpoint in this field, "closing the door" to the use of hazardous reagents and polymeric protective layers, on the production of stable copper nanowires with potential application as conductive materials.

KEYWORDS

Copper nanowires; *Eucalyptus globulus* bark; plant extracts; green synthesis; oxidative stability.

ACCEPTED MANUSCRIPT

1. Introduction

Noble metal nanostructures are among the major nanomaterial's classes, studied and used so far, because of their unique set of properties, namely optical, electrical, mechanical, and thermal (Pelaz et al., 2012). These metallic nanostructures find applications in a panoply of fields, including optical, catalytic, electronic, and medical domains (Bhanushali et al., 2015).

In particular, copper nanostructures are of enormous practical interest due to their remarkable conductive (Rathmell and Wiley, 2011), catalytic (Baig and Varma, 2013), antimicrobial (Pinto et al., 2013), and biosensing (Peng et al., 2015) properties. However, among the main limitations on the use of copper nanostructures remains on their efficient production in aqueous solutions and susceptibility towards oxidation under ambient-air conditions (Jin et al., 2011). Several studies demonstrated that amongst the various Cu nanoshapes, copper nanowires (CuNWs) present higher stability under these conditions (Pinto et al., 2012; Rathmell and Wiley, 2011).

CuNWs have been explored in several applications, for example in transparent conducting electrodes (TCE), as innovative candidates to replace high-cost indium tin oxide (ITO) in several optoelectronic devices, in particular, thin-film solar cells, flat-panel displays, and touch-screens panels due to its exceptional performance (Han et al., 2014; Ye et al., 2014). Gold (Chen et al., 2013) and silver (Cheng et al., 2015) nanowires have also demonstrated an excellent transparency/conductivity performance, nevertheless, the high cost of these noble metals is a major drawback for an industrial scale production of optoelectronic devices. This opens a unique opportunity for CuNWs since copper is 1000 times more abundant than silver (Ye et al., 2016), less expensive (100 times), higher conductor (experimental resistivity of copper at room temperature is ρ = 1.68 nΩ.m) than gold (2.44 nΩ.m) and only slightly less than silver (1.58 nΩ.m), and exhibits less susceptibility to electromigration effect when it is used in microelectronics (Chu et al., 2016; Rossiter, 1987; Xiong et al., 2011).

Several physical (*e.g.* chemical vapor deposition (Kim et al., 2008) or pulsed laser ablation (Swarnkar et al., 2016)) and chemical methodologies, namely solution-phase synthesis (*e.g.* chemical reduction (Rathmell and Wiley, 2011), seed-mediated synthesis (Mott et al., 2007) or microwave-assisted methods (Liu et al., 2012)), have been developed for the preparation of CuNWs (Bhanushali et al., 2015; Ye et al., 2016). However, solution-based methods using copper ions and appropriated reducing agents are still the most commonly used because of their simplicity, low cost, and large scalability without compromising their quality or the tuning of their dimensions (Bhanushali et al., 2015). Regarding the existing literature on this topic, it is possible to verify that hydrazine hydrate has been among the foremost reducing agent chosen for the

synthesis of this copper 1D nanostructure (Bhanushali et al., 2015; Zhang and Cui, 2009). However, the use of this molecule presents several environmental and biological risks, because it is highly toxic (Slonim, 1977). Moreover, carcinogenicity and chronic toxicity was observed in rats and mice (Matsumoto et al., 2016).

In this context, in recent years, some researchers focused their attention on the investigation of green and efficient reducing agents for the synthesis of CuNWs (Biçer and Şişman, 2010; Cho and Huh, 2009; Jin et al., 2011; Kevin et al., 2015; Li et al., 2014; Mohl et al., 2010; Panigrahi et al., 2006; Zhang et al., 2006), as well as for panoply of metal nanoparticles (Iravani, 2011; Santos et al., 2014). For instance, Zhang and co-workers (Zhang et al., 2006) developed a hydrothermal reduction strategy using ascorbic acid as the reducing agent in the presence of polyvinylpyrrolidone (PVP). Ascorbic acid acts as both the complexing and reducing agent while PVP works as polymeric protective layer against oxidation, leading to the formation of nanorods with rectangular cross-sections. Other eco-friendly methods to produce single-crystalline ultra-long CuNWs, employed glucose as reduction agent, and hexadecylamine (Mohl et al., 2010) or cetyltrimethylammonium bromide (CTAB) (Cho and Huh, 2009) as surfactant molecules. Latterly, following a similar approach, Li et al. (Li et al., 2014), using also glucose as reducing agent, demonstrated that an oleic acid/oleylamine mixture can be used as surfactants for the preparation of CuNWs via a ligand-exchange method. The combined use of these two surfactants has been advocated for stabilization purposes, however, it was also verified that impacts the size and shape of the nanostructures (Bu et al., 2009; Harris et al., 2015). It is also important to highlight that, contrary to the previously reported (Jin et al., 2011; Li et al., 2014; Mohl et al., 2010), glucose by itself does not have the capacity to reduce copper ions at hydrothermal conditions (102 ºC), as proved unequivocally by Kevin and co-workers (Kevin et al., 2015). Instead, the Maillard reaction that occurs between glucose and primary amines like oleylamine originates a multitude of compounds, some of which are responsible for the copper ions (Cu^{2+} or Cu^{+}) reduction (Kevin et al., 2015).

Despite the environmental connotation of these reducing agents, some of them are quite expensive (*e.g.*, D-(+)-Glucose ≥99.5% up to around 80 euros/kg) and need to be used in a high purification degree (Zhang et al., 2016), increasing substantially the price associated with the process. Furthermore, in some cases it is also necessary to carry out several washing steps, and/or ligand-exchange processes using, for example, PVP for exchanging of the molecules adsorbed at the surface aiming to increase dispersibility and stability of the obtained CuNWs in solution.

Regarding the biosynthesis of other metallic nanostructures, there are numerous reports focusing the employment of extracts obtained from plants, however, this approach had never been explored

for the synthesis of CuNWs. In this vein, we report here for the first time, the biosynthesis of CuNWs using a plant extract which acts simultaneously as reducing and stabilizing agent. Specifically, an *Eucalyptus globulus bark* aqueous extract was used to prepare highly stable and well-defined CuNWs by a simple, cheap, and environmentally friendly way. *E. globulus* is the main wood specie used by paper industry in several countries, including Portugal (Domingues et al., 2010). Therefore, Eucalyptus bark is an industrial residue produced in large amounts (*e.g.*, a pulp mill with a production capacity of 5.0×10^5 ton/year of bleached pulp can generate around 1.0×10^5 ton/year of bark) (Domingues et al., 2010), and therefore, obtained at low cost.

Particularly, we investigated the feasibility of the biosynthesis of CuNWs using *E. globulus* bark extract and the effect of their concentration on the size and morphology of the obtained nanostructures (Figure 1). The influence of oleylamine and oleic acid (surfactants) on the final aspect ratio of CuNWs was also evaluated. Then, insights into the biosynthesis of CuNWs using plant extracts were obtained through the use standard aqueous solutions of gallic acid and glucose, as illustrative compounds of the major families present in the *E. globulus* bark extract. Finally, the study of the stability of the obtained CuNWs towards oxidation (under storage conditions and at air exposure) was performed.

2. Experimental

2.1. Materials

Copper (II) chloride 2-hydrate (97%, Sigma-Aldrich), oleylamine (70%, Aldrich), oleic acid (90%, Aldrich), and ethanol (99.8%, Panreac) were used as received.

E. globulus bark was dried at air and then triturated until to reach a granulometry slighter than 2 mm. *E. globulus* bark extract was obtained as described by Santos et al. (Santos et al., 2014). The milled bark was subject to a water extraction 1:50 (w/v) during 2 min at a temperature of 100 °C. The resultant aqueous suspension was then filtered, and the supernatant was freeze-dried.

2.2. Biosynthesis of CuNWs

In a standard synthesis, 34.1 mg of $CuCl_2.2H_2O$ were dissolved in 4 mL of distilled water, and separately, in another beaker, 0.4 mL of oleylamine and 4 µL of oleic acid were added to 0.7 mL of ethanol under magnetic stirring. Then, the ethanol solution was added dropwise to the copper chloride solution in an Erlenmeyer and afterwards, 15.1 mL of distilled water were added. The mixture was magnetically stirred at 50 ºC for additional 12 h to promote the formation of the oleylamine-copper precursor.

Then, 1 mL of an aqueous *E. globulus* bark extract (7.5, 10, 15, 25 and 50 $mg.mL^{-1}$) was added dropwise to this mixture. Afterwards, the mixture was transferred to an autoclave (Uniclave 88) and

left to react during 2 h at 120 MPa (autoclave temperature = 121ºC). After the reaction, the CuNWs were centrifuged 10 min at 6000 rpm, sonicated and washed three times with ethanol.

In order to unveil the role of the different reactional species, namely bark extract components, oleylamine and oleic acid, similar assays using only 1 mL of an 10 $mg.mL^{-1}$ aqueous *E. globulus* bark extract (without the mixture of oleylamine/oleic acid) or in the presence of only oleylamine or oleic acid were also carried out. Furthermore, two tests with standard compounds (gallic acid and glucose) were made using 1 mL of 10 $mg.mL^{-1}$ standard compounds solutions instead of the *E. globulus* extract.

2.3. Physical and chemical characterization

The obtained CuNWs were characterized in terms of surface chemistry and composition, optical properties and crystalline structure.

The optical properties of the colloidal solutions were studied with an Evolution™ 220 UV/Visible spectrophotometer (100 $scans.min^{-1}$; bandwidth of 2.0 nm). CuNWs Fourier transform-infrared (FTIR) spectra were acquired in a Bruker optics tensor 27 spectrometer (256 scans; resolution of 4 cm^{-1}). Scanning electron microscopy (SEM) micrographs, as well as those acquired in transmission mode (STEM), were attained in a FEG-SEM Hitachi SU-70 operated at 15 kV with an energy dispersive X-ray spectroscopy (EDS) Bruker QUANTAX 400 detector. Transmission electron microscopy (TEM) pictures were attained in a FEG-TEM Jeol 2200FS and a dedicated FEG-STEM Hitachi 2700, both operated at 200 kV. The grids were obtained placing an ultra-pure water diluted drop of the obtained colloids onto the grid surface with a continuous amorphous carbon film and left to dry in air. Observation, acquisition and data analysis of the high-resolution (HR) TEM images were carried out using the Gatan Digital Micrograph software version 1.84.1282 (Gatan Inc. © 1996–2010). The width and respective length of the CuNWs was measured using Fiji software counting leastwise 100 nanowires, randomly selected in each case, using STEM and/or TEM images. X-ray photoelectron spectroscopy (XPS) spectra were acquired in an Ultra High Vacuum (UHV) system with a base pressure of $2x10^{-10}$ mbar. The system is equipped with a hemispherical electron energy analyser (SPECS Phoibos 150), a delay-line detector and a monochromatic Al Kα (1486.74 eV) X-ray source. High resolution spectra were recorded at normal emission take-off angle and with a pass-energy of 20 eV for C1s, Cu 2p and Cu LMM spectra. The binding energies obtained in XPS analysis were corrected with the reference to C 1s (284.6 eV). For XPS measurements, a drop of the sample was deposited on silicon by drop coating. The powder X-ray diffraction (XRD) patterns of the CuNWs were determined using a Philips X'Pert operated a 40 kV, 50 mA and with a CuK_α radiation (λ = 1.543178 Å). For the stability towards oxidation study, the obtained CuNWs were left in an ethanolic solution or at air outdoor conditions for 2 weeks. After this period the

XRD patterns of the two samples were measured as described above. A Rietveld refinement of the respective CuNWs prepared with glucose spectrum, when left 2 weeks under normal ambient conditions, was used to obtain the amount of copper oxide formed.

For the determination of the electrical conductivity of the CuNWs synthesized using this new methodology, they were deposited in the top of a filter paper and the electrical conductivity measured using a handmade conductivity device based on the principle of the four-point probe technique (Girotto and Santos, 2002; Seng et al., 2014).

3. Results and Discussion

3.1. Optical studies

As it is well-known, metal nanosized particles exhibit unique optical properties and CuNWs colloids are characterized by presenting a red-brown colour that indicate the reduction of the Cu^{2+} ions to Cu^{0} species (Jin et al., 2011; Kevin et al., 2015; Li et al., 2014).

In this work, adding later the *E. globulus* Labill. bark aqueous extract to the cyan oleylamine-copper precursor solution (Figure 2a), a greyish brown colour (Figure 2b) was observed, and after the hydrothermal reduction reaction, the colloid acquired a red brick colour, as shown in Figure 2c, giving a first indication of the success of the reduction reaction (Ahn et al., 2015; Cui et al., 2015; Liu et al., 2012).

However, it was verified that the visual formation of CuNWs only occurred for *E. globulus* aqueous extracts concentrations higher than 10 $mg.mL^{-1}$ (S.I. Fig S1). When a lower concentration (7.5 $mg.mL^{-1}$) was used, the final colloid does not present a red-like colour indicating that, in this case, CuNWs were not formed (Ahn et al., 2015; Cui et al., 2015; Liu et al., 2012). This clearly demonstrated that the extract concentration used plays a key role in this biosynthetic approach. A similar behaviour was verified by Kevin et al. (Kevin et al., 2015) and Zhang et al. (Zhang et al., 2006) using glucose and ascorbic acid as reducing agents, respectively. The need of a high number of reduction species, formed *in situ*, for the reduction of copper ions into CuNWs instead of other copper species can be one of the reasons for this behaviour as referred by these authors. Nevertheless, it is important to highlight that in this synthesis the mass relation between the *E. globulus* extract and the copper salt used is lower than the mass balance usually required for other reducing agents (Kevin et al., 2015; Zhang et al., 2006).

Additionally, two independent assays using oleylamine and oleic acid separately were also carried out. The addition of oleylamine alone to the copper salt solution also caused a colour change to blue-green, confirming the formation of the copper complex (S.I. Fig S2). However, the single addition of oleic acid does not lead to this colour change. Consecutively, after the biosynthesis using the *E. globulus* extract, the

formation of CuNWs (formation of a red brick colloid) was only perceived when oleylamine was used. Moreover, the bark extract alone (without oleylamine or the mixture of oleylamine/oleic acid) was also not able to produce CuNWs. These results clearly indicate that oleylamine plays a central role on the formation of copper complexes and consequently on their reduction using this plant extract.

Figure 3 displays the UV−vis absorption spectra of the aqueous colloids of the CuNWs obtained using different *E. globulus* concentrations (10, 15, 25 and 50 $mg.mL^{-1}$) and of the pristine *E. globulus* extract for comparison purposes. The spectroscopic analysis has proved to be very useful to study metal nanostructures because the peak positions and shapes are sensitive to their size (Xiong et al., 2011). For all the extract concentration, a shoulder peak located at 580-615 nm region was observed, which agreed with values previously reported for CuNWs aqueous colloids (Li et al., 2014; Yang et al., 2014).

It was also perceived that the position of the localized surface plasmon resonance peak (LSPR) of the CuNWs swifts from 584 to 613 nm when the extract concentration increased from 10 to 50 $mg.mL^{-1}$, respectively. This red shift could indicate the formation of longer CuNWs (Yang et al., 2014). Furthermore, the use of a high extract concentration led to the formation of a broader absorption peak, suggesting a wide size distribution and/or the presence of Cu nanostructures with other morphologies. As described by several authors, the molecules that are present in these bioextracts can act in a dual role, working as reducing and stabilizing compounds, during the biosynthesis of metallic nanostructures. Along this growth, Ostwald ripening could take place and result in the broadening of the size distribution, justifying the attainment of a more broad absorption band (Santos et al., 2014; Sharma et al., 2009). In fact, the optical spectra displayed in Figure 3 also shows that the CuNWs prepared with the higher extract concentration presented a larger amount of extract biomolecules at their surface due to the presence of a more intense absorption in the 250-300 nm region that is characteristic of the *E. globulus* aqueous extract.

3.2. FTIR characterization

To further confirm the presence of biomolecules from the extract at the CuNWs surface, the samples were then characterized by FTIR spectroscopy. Figure 4 shows the FTIR spectra of the CuNWs synthetized with distinct *E. globulus* concentrations, as well as the spectrum of the initial extract.

The pristine *E. globulus* aqueous bark extract spectrum showed numerous absorption bands, usually between 1000 and 1800 cm^{-1}, that were attributed to the vibrations of characteristic functional groups from some water-soluble components present in this aqueous extract (specifically sugars and phenolic compounds) (Santos et al., 2014). In the FTIR spectra of the biosynthesized CuNWs, it was possible to see some of these bands, confirming undoubtedly that some of those biomolecules are at the CuNWs surface working as capping agents, helping in the stabilization of these nanostructures in solution. These results corroborate those of the UV-vis analysis.

The spectra of the CuNWs samples showed also a small band at 3011 cm^{-1} corresponding to the stretching of =C-H bonds and two sharp bands at 2857 and 2926 cm^{-1} that are attributed to the CH_2 symmetric and asymmetric stretching vibrations, respectively (Limaye et al., 2009). This observation indicates the presence of some remaining oleyl groups passivating also the surface of the formed CuNWs. Similarly, $CoFe_2O_4$ (Limaye et al., 2009), and Fe_3O_4 NPs synthesised using oleylamine also showed oleyl groups on their surface (Harris et al., 2015; Wilson and Langell, 2014).

3.3. XRD analysis

The crystalline structure of the CuNWs was examined using XRD. Figure 5 shows the typical XRD pattern of the as-formed nanowires. The three characteristic peaks, located at 2θ = 43.2°, 50.4°, and 74.1°, can be indexed to the reflections of the {111}, {200}, and {220} planes of face-centered cubic (fcc) structured Cu (ICDD 04-010-6011).

Most importantly, it can be observed that oxidation of the CuNWs did not take place since no characteristic peaks of the most common copper oxides polymorphs were detected in the obtained XRD pattern. Likewise, it was not perceived the presence of residual copper (I) (CuCl - nantokite, with typical reflections around 28°, 47° and 56° of 2θ), which clearly indicates that the reduction of the initial precursor Cu(II) to Cu(0) was complete. In sum, XRD results indicate that only metal copper products were obtained under the current synthetic conditions.

3.4. Size and morphology analysis

SEM and TEM were used to study the morphology and size distribution of the biosynthesized nanowires. Figure 6 shows the SEM images of the CuNWs formed after 2 h of reaction in the autoclave using 10 and 15 $mg.mL^{-1}$ of *E. globulus* extract.

In both cases, the colloid is composed mainly of nanowires, however, small amounts of particle-like nanomaterial as nanospheres, nanoprisms and nanocubes were observed (S.I. Fig. S3). The successful formation of the CuNWs was also confirmed by EDS and respective mapping (S.I. Fig. S4). It can be verified that when the concentration of *E. globulus* was increased (particularly for 25 and 50 $mg.mL^{-1}$) the number of spherical particles and the agglomeration of the CuNWs also increases. A similar behaviour has been verified when high concentrations of glucose were used in the synthesis of these nanostructures (Mohl et al., 2010; Panigrahi et al., 2006). This fact was explained based on the high concentration of the reduction agent that allows the formation of a great number of seeds (Kim et al., 2017; Luo et al., 2016). In literature, it is accepted that the synthesis of Cu NWs followed a seed-mediated growth (Kim et al., 2017; Luo et al., 2016). In other words, the

synthesis follows two discrete steps, the first step is devoted to the production of seeds and in the second one, the seeds act as nucleation sites to generate the desired nanocrystals. The concentration of the initial "seed" clusters is influenced by the amount of the reducing agent used, which in turn determines the total number of resulting particles. Therefore, higher extract concentration resulted in a higher number of seeds. The formation of a large number of seeds will slow down the growth rate and the amount of copper ions in solution available to participate in the wire growth (Thanh et al., 2014).

The obtained CuNWs presented an average diameter of 44±8, 65±13, 125±28, and 145±22 nm for extract concentrations from 10 to 50 $mg.mL^{-1}$, respectively. These results are in perfect accordance with the UV-vis results that indicated a broadening of the absorption band for higher extract concentrations. The lengths of the CuNWs varied from 5 to dozens of micrometres (S.I. Fig.S5). However, when compared with those obtained when using only oleylamine and the same concentration of extract (10 $mg.mL^{-1}$), a significant difference on the size of the nanostructures was observed (Figure 7).

It is possible to observe that the obtained CuNWs are ticker (≈500 nm) and relatively shorter (7-10 µm) indicating that oleic acid, despite the fact that does not allow the formation of the CuNWs when used alone, has a crucial impact on their size. The important role of oleic acid as structure-directing agent was already reported for anisotropic structures as bipyramidal rhombic (Bu et al., 2009), and dog-bone nanocrystals (Dinh et al., 2009). CuNWs with an aspect ratio of 14-20 were obtained in this case, values significantly lower than those observed when using the mixture oleylamine/oleic acid (160-400) and the same *E. globulus* concentration (10 $mg.mL^{-1}$).

3.5. HR-TEM analysis

The micro and nanostructure of the CuNWs were further studied by HR-TEM, as seen in Figure 8. Figure 8a clearly confirms the morphology of the CuNWs obtained by reduction with the *E. globulus* extract, as well as the previously discussed average diameter and length. Additionally, HR-TEM images (Figure 8b and Figure 8c) markedly show the biomolecules layer surrounding the obtained CuNWs, as well as that they preferentially grow along the {1,1,1} axis direction, as seen in Figure 8b. This thin layer around the CuNWs is probably due to the presence of some components present in the *E. globulus* extract, as phenolic compounds and/or sugars adsorbed at their surface. This agrees with previously reported works, regarding the biosynthesis of other types of metallic nanostructures, particularly nanoparticles that described the dual reducing and protective role of the water-soluble biomolecules present in plant extracts (Huang et al., 2015; Sharma et al., 2009). This is also consistent with the results of the optical (Figure 3) and FTIR analysis (Figure 4). In Figure 8b,

the crystalline fringes of 2.06 Å and 1.26 Å were identified for the {1,1,1} and {2,2,0} of Cu, respectively. The slight differences observed for the dhkl values are acceptable and consistent with those for Cu, bearing in mind that the HR-TEM images measurements are inevitably affected by the presence of the continuous amorphous carbon film. In HR-TEM analysis, no evidence of oxidation of the CuNWs was observed. Thus, these findings are also in excellent agreement with the XRD patterns observed for the obtained metallic copper NWs (Figure 5). The inset in Figure 8b showing the FFT electron diffraction image obtained in that region enabled the identification of the {1,1,1}, {2,2,0} and {2,0,0} crystalline planes around the [-1,1,0] zone axis. HR-TEM analysis of the CuNWs end edge (Figure 8c) also revealed crystalline fringes corresponding to the {1,1,1}, {2,0,0} and {2,2,0} planes of Cu. Although axis rotation was not performed during HR-TEM images acquisition, based on these results we can conclude that the CuNWs apparently present a penta-twinned structure bound by {111} facets at the two ends, which is highly consistent with previously reported results for CuNWs, as well as for other metals including Ag (Sun et al., 2003) or Au (Johnson et al., 2002).

3.6. XPS analysis

The surface characterization of the freshly obtained CuNWs was carried out by XPS as shown in Figure 9 and Figure S6. The XPS analysis reveal the presence of C, O, and Cu as the major elements present in the surface of the CuNWs. These results suggest that phenolic compounds and sugars, initially present on the extract, or their derivatives formed during the CuNWs synthesis, are adsorbed at the surface of the CuNWs.

Additionally, in the C 1s region, the high resolution XPS spectrum of biosynthesized CuNWs showed the characteristic peaks of sp^3/sp^2 carbon at lower biding energies (284.6 eV), the C-C and C-H contribution (285.3), the ether (C-O-C) and hydroxylic (C-OH) contributing (285.9 eV), and the carbonyl (C=O) and the oxidized carbon (O-C=O) contributing at higher binding energies (287.8 eV) (Santos et al., 2018).

In the Cu 2p spectrum, two strong peaks are observed at 932.9 and 952.8 eV, corresponding to Cu $2p_{1/2}$ and Cu $2p_{3/2}$ (Chen et al., 2010). The peak position, line-shape and peak-to-peak separation of the Cu doublet (19.9 eV) was consistent with the reported data for Cu zero state (Chang et al., 2005; Chen et al., 2010). The Gaussian deconvolution of the Cu $2p_{1/2}$ and Cu $2p_{3/2}$ peaks showed two peaks at 935.7 and at 955.4 eV that can indicate the presence of small amounts of copper oxide (CuO and Cu_2O) at the surface of the CuNWs. The Cu LMM spectrum confirm this fact showing not only the presence of Cu(0) (peak at ≈568.0 eV) but also the presence of CuO (≈569.0 eV) and Cu_2O (≈569.8 eV) peaks (Aria et al., 2016). These results are not in based on the distinct experimental working principles, namely the penetration

depth of the incident radiation is different in both cases. Therefore, in XPS even very small fractions of copper oxides can be detected in the outer surface of CuNWs, contrary to XRD analysis.

3.7. Insights into the biosynthesis of CuNWs using plant extracts

To understand the reducing ability of some of the main phenolic compounds and sugars present in the *E. globulus* aqueous extract (Santos et al., 2014), in the CuNWs biosynthesis, standard solutions of gallic acid and glucose were tested separately as reducing agents. Following this procedure, it was verified that the use of both standard compounds allowed the formation of CuNWs, as verified by the appearance of the corresponding UV absorption band with $\lambda_{máx}$ at 584 nm (S.I. Fig.S7). This behaviour suggests that, in this case, when a natural extract is used, sugars (as glucose) cannot be addressed as the only compounds responsible for the reduction of Cu^{2+} and the chemical reactions behind the formation CuNWs cannot be completely addressed to the occurrence of Maillard reactions involving reducing sugars, as glucose (Kevin et al., 2015). The presence of HO- and -COOH groups in the structure of phenolic compounds, as gallic acid and correspondent derivatives, can allow their interaction with the Cu ions, causing the oxidation of these groups and promoting the copper ions reduction, leading to the formation of the metal nanostructures (Santos et al., 2014). This is a clear validation that the biosynthesis of Cu nanostructures using a natural extract is a more complex process involving different biomolecules, namely phenolic compounds and sugars.

An important aspect is that the CuNWs obtained using the gallic acid standard solution practically do not present additionally particle-like nanostructures, as in the case of the standard glucose solution and *E. globulus* bark extract (Figure 10). The fine-tuning of the size and shape of nanostructures is a key aspect regarding their properties and, therefore, this work opens a new vision in the green synthesis of CuNWs with tuned sizes and morphologies.

3.8. Study of CuNWs air-oxidation

To assess the oxidation "protective" role of the extract biomolecules adsorbed onto the Cu nanostructures during the biosynthesis, CuNWs were left to stand during 2 weeks in ambient conditions and in an ethanolic solution (Figure 11). As the same time, CuNWs prepared following the same experimental procedure, but using glucose as reducing agent, were also submitted to the same storage conditions to study their oxidation behaviour for comparative purposes. The XRD diffraction patterns of CuNWs prepared with *E. globulus* extract after exposure to air for 2 weeks show that, for both conditions tested, the three characteristic peaks of CuNWs were maintained and there was no clear evidence of diffractions of CuO or Cu_2O in the powder XRD of the analysed samples. When the CuNWs prepared with glucose were left in the ethanolic solution, it was not verified the related oxide phases appearance.

However, when left in normal ambient conditions, after the 2 weeks, the appearance of the characteristic peaks of Cu_2O phase was clear. Using Rietveld refinement, a percentage of 10.3% for cuprite phase was obtained.

In this sense, it is clear that *E. globulus* biomolecules display a significant protective role against air oxidation of CuNWs. This behaviour can be explained based on the chemical composition of the aqueous *E. globulus* extract used on the biosynthesis. As described before by our group (Santos et al., 2014), when this extract is used for the biosynthesis of Au and Ag NPs, phenolic compounds, as ellagic acid and isorhamnetin, are the main responsible for the reduction and stabilization of the nanostructures. These two biomolecules are well-known for presenting a significant antioxidant activity and, as other components from this family typically present in this aqueous extract, and therefore can play a decisive role in preventing the air oxidation of CuNWs (Santos et al., 2013, 2012; Srivastava et al., 2007).

Previous methodologies to prepare NWs, including those using glucose as reducing agent (Li et al., 2014; Mohl et al., 2010), requires the use of PVP to prevent the agglomeration and as a protective layer (capping agent) of this nanostructure, and in some cases to retard the oxidation of copper (Kevin et al., 2015). However, as-prepared CuNWs are not conductive unless this polymer layer is removed at high temperatures and in an inert medium.

In order to confirm the advantage of this methodology, the conductivity of the obtained CuNWs was measured using the four-point probe technique (Girotto and Santos, 2002; Seng et al., 2014), and it was found to be 0.09 $S.cm^{-1}$. The conductivity value obtained is slightly lower than that described in literature for materials based in copper nanowires (*e.g.* CuNWs-PVA aerogel-based conductors, 0.83 $S.cm^{-1}$ (Tang et al., 2014), and ultralow-density copper nanowire aerogel monoliths, 0.90 to 1.76 $S.cm^{-1}$ (Tang et al., 2013)). This difference can be explained based on several experimental parameters (including temperature and experimental set-up) as well as on the fact that the obtained CuNWs also contain other Cu nanostructures, namely Cu nanospheres (Kang et al., 2018).

4. Conclusions

CuNWs have been successfully obtained by a new and simple biosynthetic methodology using *E. globulus* extract as reducing and protecting agent. The extract concentration plays a key role in the formation of these nanostructures allowing to control their dimensions and morphologies. The addition of oleic acid to the reactional mixture allows to prepare CuNWs with larger aspect ratios. The assays with standard compounds (gallic acid and glucose) showed that the reduction behaviour of this extract cannot be simply addressed to sugars, but phenolics compounds as gallic acid (and derivatives) have also this ability.

Finally, we provided compelling evidence that the obtained CuNWs present a significant resistance to air oxidation, not presenting copper oxide phases after 2 weeks, due to the adsorption of antioxidant extract biomolecules at their surface. With this approach, no addition of polymeric layer after the CuNWs synthesis was needed which could represent an enormous technological advantage when considering electrical conduction applications of this type of nanostructures. The implementation of this methodology will allow reducing the cost of production of CuNWs because the components of the extract acts as the reducing agent and as the protective layer and the additional step to remove the protective polymeric layer is also avoided. The biobased CuNWs presented a conductivity of 0.009 $S.cm^{-1}$ (four-point probe technique). However, in the future, it will be important to validate these results using other plant extracts, and by preparing materials using these promising CuNWs.

Furthermore, this work could open a new range of possibilities in this field for the "green" tuning of CuNWs dimensions/shapes and, at same time, the surface chemistry, via use of different plant extracts and/or plant extracts enriched in phenolic compounds.

ACKNOWLEDGEMENTS

This work was developed within the scope of the project CICECO-Aveiro Institute of Materials, FCT (Fundação para a Ciência e a Tecnologia, I.P.) Ref. UID/CTM/50011/2019, financed by national funds through the FCT/MCTES. The costs resulting from the FCT hiring of R.J.B. Pinto is funded by national funds (OE), through FCT, in the scope of the framework contract foreseen in the numbers 4, 5 and 6 of the article 23, of the Decree-Law 57/2016, of August 29, changed by Law 57/2017, of July 19. A.V. Girão wish to thank the Scientific Project Portugal 2020 FEDER-POCI *ProDiam – Productivity increase with CVD diamond coated tools*. C.S.R. Freire and P.A.A.P. Marques also acknowledge the FCT/MCTES for the investigation contracts (Program Investigador FCT 2012 IF/01407/2012 and 2013 IF/00917/2013/CP1162/CT0016, respectively). Microscopy was maintained by the Rede Nacional de Microscopia Eletrónica, project REDE/1509/RME/2005.

REFERENCES

Ahn, Y., Jeong, Y., Lee, D., Lee, Y., 2015. Copper Nanowire–Graphene Core–Shell Nanostructure for Highly Stable Transparent Conducting Electrodes. ACS Nano 9, 3125–3133. https://doi.org/10.1021/acsnano.5b00053

Aria, A.I., Kidambi, P.R., Weatherup, R.S., Xiao, L., Williams, J.A., Hofmann, S., 2016. Time Evolution of the Wettability of Supported Graphene under Ambient Air Exposure. J. Phys. Chem. C 120,

2215–2224. https://doi.org/10.1021/acs.jpcc.5b10492

Baig, R.B.N., Varma, R.S., 2013. Copper on chitosan: a recyclable heterogeneous catalyst for azide–alkyne cycloaddition reactions in water. Green Chem. 15, 1839. https://doi.org/10.1039/c3gc40401c

Bhanushali, S., Ghosh, P., Ganesh, A., Cheng, W., 2015. 1D Copper Nanostructures: Progress, Challenges and Opportunities. Small 11, 1232–1252. https://doi.org/10.1002/smll.201402295

Biçer, M., Şişman, I., 2010. Controlled synthesis of copper nano/microstructures using ascorbic acid in aqueous CTAB solution. Powder Technol. 198, 279–284. https://doi.org/10.1016/j.powtec.2009.11.022

Bu, W., Chen, Z., Chen, F., Shi, J., 2009. Oleic Acid/Oleylamine Cooperative-Controlled Crystallization Mechanism for Monodisperse Tetragonal Bipyramid NaLa(MoO4)2 Nanocrystals. J. Phys. Chem. C 113, 12176–12185. https://doi.org/10.1021/jp901437a

Chang, Y., Lye, M.L., Zeng, H.C., 2005. Large-Scale Synthesis of High-Quality Ultralong Copper Nanowires. Langmuir 21, 3746–3748. https://doi.org/10.1021/la050220w

Chen, H., Lee, J.-H., Kim, Y.-H., Shin, D.-W., Park, S.-C., Meng, X., Yoo, J.-B., 2010. Metallic Copper Nanostructures Synthesized by a Facile Hydrothermal Method. J. Nanosci. Nanotechnol. 10, 629–636. https://doi.org/10.1166/jnn.2010.1739

Chen, Y., Ouyang, Z., Gu, M., Cheng, W., 2013. Mechanically Strong, Optically Transparent, Giant Metal Superlattice Nanomembranes From Ultrathin Gold Nanowires. Adv. Mater. 25, 80–85. https://doi.org/10.1002/adma.201202241

Cheng, Y., Wang, R., Sun, J., Gao, L., 2015. Highly Conductive and Ultrastretchable Electric Circuits from Covered Yarns and Silver Nanowires. ACS Nano 9, 3887–3895. https://doi.org/10.1021/nn5070937

Cho, Y.-S., Huh, Y.-D., 2009. Synthesis of ultralong copper nanowires by reduction of copper-amine complexes. Mater. Lett. 63, 227–229. https://doi.org/10.1016/j.matlet.2008.09.049

Chu, H.-C., Chang, Y.-C., Lin, Y., Chang, S.-H., Chang, W.-C., Li, G.-A., Tuan, H.-Y., 2016. Spray-Deposited Large-Area Copper Nanowire Transparent Conductive Electrodes and Their Uses for Touch Screen Applications. ACS Appl. Mater. Interfaces 8, 13009–13017. https://doi.org/10.1021/acsami.6b02652

Cui, F., Yu, Y., Dou, L., Sun, J., Yang, Q., Schildknecht, C., Schierle-Arndt, K., Yang, P., 2015. Synthesis of Ultrathin Copper Nanowires Using Tris(trimethylsilyl)silane for High-Performance and Low-Haze Transparent Conductors. Nano Lett. 15, 7610–7615. https://doi.org/10.1021/acs.nanolett.5b03422

Dinh, C.-T., Nguyen, T.-D., Kleitz, F., Do, T.-O., 2009. Shape-Controlled Synthesis of Highly Crystalline Titania Nanocrystals. ACS Nano 3, 3737–3743. https://doi.org/10.1021/nn900940p

Domingues, R.M.A., Sousa, G.D.A., Freire, C.S.R., Silvestre, A.J.D., Neto, C.P., 2010. Eucalyptus globulus biomass residues from pulping industry as a source of high value triterpenic compounds. Ind. Crops Prod. 31, 65–70. https://doi.org/10.1016/j.indcrop.2009.09.002

Girotto, E.M., Santos, I.A., 2002. Medidas de resistividade elétrica DC em sólidos: como efetuálas corretamente. Quim. Nova 25, 639–647. https://doi.org/10.1590/S0100-40422002000400019

Han, S., Hong, S., Ham, J., Yeo, J., Lee, J., Kang, B., Lee, P., Kwon, J., Lee, S.S., Yang, M.-Y., Ko, S.H., 2014. Fast Plasmonic Laser Nanowelding for a Cu-Nanowire Percolation Network for Flexible Transparent Conductors and Stretchable Electronics. Adv. Mater. 26, 5808–5814. https://doi.org/10.1002/adma.201400474

Harris, R.A., Shumbula, P.M., van der Walt, H., 2015. Analysis of the Interaction of Surfactants Oleic Acid and Oleylamine with Iron Oxide Nanoparticles through Molecular Mechanics Modeling. Langmuir 31, 3934–3943. https://doi.org/10.1021/acs.langmuir.5b00671

Huang, J., Lin, L., Sun, D., Chen, H., Yang, D., Li, Q., 2015. Bio-inspired synthesis of metal nanomaterials and applications. Chem. Soc. Rev. 44, 6330–6374. https://doi.org/10.1039/C5CS00133A

Iravani, S., 2011. Green synthesis of metal nanoparticles using plants. Green Chem. 13, 2638. https://doi.org/10.1039/c1gc15386b

Jin, M., He, G., Zhang, H., Zeng, J., Xie, Z., Xia, Y., 2011. Shape-Controlled Synthesis of Copper Nanocrystals in an Aqueous Solution with Glucose as a Reducing Agent and Hexadecylamine as a Capping Agent. Angew. Chemie Int. Ed. 50, 10560–10564. https://doi.org/10.1002/anie.201105539

Johnson, C.J., Dujardin, E., Davis, S.A., Murphy, C.J., Mann, S., 2002. Growth and form of gold nanorods prepared by seed-mediated, surfactant-directed synthesis. J. Mater. Chem. 12, 1765–1770. https://doi.org/10.1039/b200953f

Kang, C., Yang, S., Tan, M., Wei, C., Liu, Q., Fang, J., Liu, G., 2018. Purification of Copper Nanowires To Prepare Flexible Transparent Conductive Films with High Performance. ACS Appl. Nano Mater. 1, 3155–3163. https://doi.org/10.1021/acsanm.8b00326

Kevin, M., Lim, G.Y.R., Ho, G.W., 2015. Facile control of copper nanowire dimensions via the Maillard reaction: using food chemistry for fabricating large-scale transparent flexible conductors. Green Chem. 17, 1120–1126. https://doi.org/10.1039/C4GC01566E

Kim, C., Gu, W., Briceno, M., Robertson, I.M., Choi, H., Kim, K. (Kevin), 2008. Copper Nanowires with a Five-Twinned Structure Grown by Chemical Vapor Deposition. Adv. Mater. 20, 1859–1863. https://doi.org/10.1002/adma.200701460

Kim, H., Choi, S.-H., Kim, M., Park, J.-U., Bae, J., Park, J., 2017. Seed-mediated synthesis of ultra-long copper nanowires and their application as transparent conducting electrodes. Appl. Surf. Sci. 422, 731–737. https://doi.org/10.1016/j.apsusc.2017.06.051

Li, S., Chen, Y., Huang, L., Pan, D., 2014. Large-Scale Synthesis of Well-Dispersed Copper Nanowires in an Electric Pressure Cooker and Their Application in Transparent and Conductive Networks. Inorg. Chem. 53, 4440–4444. https://doi.org/10.1021/ic500094b

Limaye, M. V., Singh, S.B., Date, S.K., Kothari, D., Reddy, V.R., Gupta, A., Sathe, V., Choudhary, R.J., Kulkarni, S.K., 2009. High Coercivity of Oleic Acid Capped CoFe 2 O 4 Nanoparticles at Room Temperature. J. Phys. Chem. B 113, 9070–9076. https://doi.org/10.1021/jp810975v

Liu, Y.-Q., Zhang, M., Wang, F.-X., Pan, G.-B., 2012. Facile microwave-assisted synthesis of uniform single-crystal copper nanowires with excellent electrical conductivity. RSC Adv. 2, 11235. https://doi.org/10.1039/c2ra21578k

Luo, M., Ruditskiy, A., Peng, H.-C., Tao, J., Figueroa-Cosme, L., He, Z., Xia, Y., 2016. Penta-Twinned Copper Nanorods: Facile Synthesis via Seed-Mediated Growth and Their Tunable Plasmonic Properties. Adv. Funct. Mater. 26, 1209–1216. https://doi.org/10.1002/adfm.201504217

Matsumoto, M., Kano, H., Suzuki, M., Katagiri, T., Umeda, Y., Fukushima, S., 2016. Carcinogenicity and chronic toxicity of hydrazine monohydrate in rats and mice by two-year drinking water treatment. Regul. Toxicol. Pharmacol. 76, 63–73. https://doi.org/10.1016/j.yrtph.2016.01.006

Mohl, M., Pusztai, P., Kukovecz, A., Konya, Z., Kukkola, J., Kordas, K., Vajtai, R., Ajayan, P.M., 2010. Low-Temperature Large-Scale Synthesis and Electrical Testing of Ultralong Copper Nanowires †.

Langmuir 26, 16496–16502. https://doi.org/10.1021/la101385e

Mott, D., Galkowski, J., Wang, L., Luo, J., Zhong, C.-J., 2007. Synthesis of Size-Controlled and Shaped Copper Nanoparticles. Langmuir 23, 5740–5745. https://doi.org/10.1021/la0635092

Panigrahi, S., Kundu, S., Ghosh, S.K., Nath, S., Praharaj, S., Basu, S., Pal, T., 2006. Selective one-pot synthesis of copper nanorods under surfactantless condition. Polyhedron 25, 1263–1269. https://doi.org/10.1016/j.poly.2005.09.006

Pelaz, B., Jaber, S., de Aberasturi, D.J., Wulf, V., Aida, T., de la Fuente, J.M., Feldmann, J., Gaub, H.E., Josephson, L., Kagan, C.R., Kotov, N.A., Liz-Marzán, L.M., Mattoussi, H., Mulvaney, P., Murray, C.B., Rogach, A.L., Weiss, P.S., Willner, I., Parak, W.J., 2012. The state of nanoparticle-based nanoscience and biotechnology: progress, promises, and challenges. ACS Nano 6, 8468–8483. https://doi.org/10.1021/nn303929a

Peng, F., Liu, Z., Li, W., Huang, Y., Nie, Z., Yao, S., 2015. Enzymatically generated long polyT-templated copper nanoparticles for versatile biosensing assay of DNA-related enzyme activity. Anal. Methods 7, 4355–4361. https://doi.org/10.1039/C5AY00423C

Pinto, R.J.B., Daina, S., Sadocco, P., Neto, C.P., Trindade, T., 2013. Antibacterial Activity of Nanocomposites of Copper and Cellulose. Biomed Res. Int. 2013, 1–6. https://doi.org/10.1155/2013/280512

Pinto, R.J.B., Neves, M.C., Neto, C.P., Trindade, T., 2012. Growth and Chemical Stability of Copper Nanostructures on Cellulosic Fibers. Eur. J. Inorg. Chem. 2012, 5043–5049. https://doi.org/10.1002/ejic.201200605

Rathmell, A.R., Wiley, B.J., 2011. The Synthesis and Coating of Long, Thin Copper Nanowires to Make Flexible, Transparent Conducting Films on Plastic Substrates. Adv. Mater. 23, 4798–4803. https://doi.org/10.1002/adma.201102284

Rossiter, P.L., 1987. Electrical resistivity of simple metals and alloys, in: The Electrical Resistivity of Metals and Alloys, Cambridge Solid State Science Series. Cambridge University Press, Cambridge, pp. 137–271. https://doi.org/10.1017/CBO9780511600289.006

Santos, C.I.M., Mariz, I.F.A., Pinto, S.N., Gonçalves, G., Bdikin, I., Marques, P.A.A.P., Neves, M.G.P.M.S., Martinho, J.M.G., Maçôas, E.M.S., 2018. Selective two-photon absorption in carbon dots: a piece of the photoluminescence emission puzzle. Nanoscale 10, 12505–12514.

https://doi.org/10.1039/C8NR03365J

Santos, S.A.O., Pinto, R.J.B., Rocha, S.M., Marques, P.A.A.P., Neto, C.P., Silvestre, A.J.D., Freire, C.S.R., 2014. Unveiling the Chemistry behind the Green Synthesis of Metal Nanoparticles. ChemSusChem 7, 2704–2711. https://doi.org/10.1002/cssc.201402126

Santos, S.A.O., Villaverde, J.J., Silva, C.M., Neto, C.P., Silvestre, A.J.D., 2012. Supercritical fluid extraction of phenolic compounds from Eucalyptus globulus Labill bark. J. Supercrit. Fluids 71, 71–79. https://doi.org/10.1016/j.supflu.2012.07.004

Santos, S.A.O., Villaverde, J.J., Sousa, A.F., Coelho, J.F.J., Neto, C.P., Silvestre, A.J.D., 2013. Phenolic composition and antioxidant activity of industrial cork by-products. Ind. Crops Prod. 47, 262–269. https://doi.org/10.1016/j.indcrop.2013.03.015

Seng, S., Shinpei, T., Yoshihiko, I., Masakazu, K., 2014. Development of a Handmade Conductivity Measurement Device for a Thin-Film Semiconductor and Its Application to Polypyrrole. J. Chem. Educ. 91, 1971–1975. https://doi.org/10.1021/ed500287q

Sharma, V.K., Yngard, R.A., Lin, Y., 2009. Silver nanoparticles: Green synthesis and their antimicrobial activities. Adv. Colloid Interface Sci. 145, 83–96. https://doi.org/10.1016/j.cis.2008.09.002

Slonim, A.R., 1977. Acute toxicity of selected hydrazines to the common guppy. Water Res. 11, 889–895. https://doi.org/10.1016/0043-1354(77)90077-X

Srivastava, A., Jagan Mohan Rao, L., Shivanandappa, T., 2007. Isolation of ellagic acid from the aqueous extract of the roots of Decalepis hamiltonii: Antioxidant activity and cytoprotective effect. Food Chem. 103, 224–233. https://doi.org/10.1016/j.foodchem.2006.08.010

Sun, Y., Mayers, B., Herricks, T., Xia, Y., 2003. Polyol Synthesis of Uniform Silver Nanowires: A Plausible Growth Mechanism and the Supporting Evidence. Nano Lett. 3, 955–960. https://doi.org/10.1021/nl034312m

Swarnkar, R.K., Pandey, J.K., Soumya, K.K., Dwivedi, P., Sundaram, S., Prasad, S., Gopal, R., 2016. Enhanced antibacterial activity of copper/copper oxide nanowires prepared by pulsed laser ablation in water medium. Appl. Phys. A 122, 704. https://doi.org/10.1007/s00339-016-0232-3

Tang, Y., Gong, S., Chen, Y., Yap, L.W., Cheng, W., 2014. Manufacturable Conducting Rubber Ambers and Stretchable Conductors from Copper Nanowire Aerogel Monoliths. ACS Nano 8, 5707–5714. https://doi.org/10.1021/nn502702a

Tang, Y., Yeo, K.L., Chen, Y., Yap, L.W., Xiong, W., Cheng, W., 2013. Ultralow-density copper nanowire aerogel monoliths with tunable mechanical and electrical properties. J. Mater. Chem. A 1, 6723. https://doi.org/10.1039/c3ta10969k

Thanh, N.T.K., Maclean, N., Mahiddine, S., 2014. Mechanisms of Nucleation and Growth of Nanoparticles in Solution. Chem. Rev. 114, 7610–7630. https://doi.org/10.1021/cr400544s

Wilson, D., Langell, M.A., 2014. XPS analysis of oleylamine/oleic acid capped Fe3O4 nanoparticles as a function of temperature. Appl. Surf. Sci. 303, 6–13. https://doi.org/10.1016/j.apsusc.2014.02.006

Xiong, J., Wang, Y., Xue, Q., Wu, X., 2011. Synthesis of highly stable dispersions of nanosized copper particles using l-ascorbic acid. Green Chem. 13, 900. https://doi.org/10.1039/c0gc00772b

Yang, H.-J., He, S.-Y., Tuan, H.-Y., 2014. Self-Seeded Growth of Five-Fold Twinned Copper Nanowires: Mechanistic Study, Characterization, and SERS Applications. Langmuir 30, 602–610. https://doi.org/10.1021/la4036198

Ye, S., Rathmell, A.R., Chen, Z., Stewart, I.E., Wiley, B.J., 2014. Metal Nanowire Networks: The Next Generation of Transparent Conductors. Adv. Mater. 26, 6670–6687. https://doi.org/10.1002/adma.201402710

Ye, S., Stewart, I.E., Chen, Z., Li, B., Rathmell, A.R., Wiley, B.J., 2016. How Copper Nanowires Grow and How To Control Their Properties. Acc. Chem. Res. 49, 442–451. https://doi.org/10.1021/acs.accounts.5b00506

Zhang, X.-F., Liu, Z.-G., Shen, W., Gurunathan, S., 2016. Silver Nanoparticles: Synthesis, Characterization, Properties, Applications, and Therapeutic Approaches. Int. J. Mol. Sci. 17, 1534. https://doi.org/10.3390/ijms17091534

Zhang, X., Cui, Z., 2009. Synthesis of Cu nanowires via solventhermal reduction in reverse microemulsion system. J. Phys. Conf. Ser. 152, 012022. https://doi.org/10.1088/1742-6596/152/1/012022

Zhang, X., Zhang, D., Ni, X., Zheng, H., 2006. One-step preparation of copper nanorods with rectangular cross sections. Solid State Commun. 139, 412–414. https://doi.org/10.1016/j.ssc.2006.06.042

ACCEPTED MANUSCRIPT

ACCEPTED MANUSCRIPT

Figure Captions

Figure 1 – Schematic overview of the CuNWs biosynthesis using *E. globulus* bark extract.

Figure 2 – Digital images of the a) initial oleylamine-copper precursor, b) solution after the addition of *E. globulus* extract and c) final colloid containing the CuNWs.

Figure 3– UV-vis spectra of the aqueous solutions of *E. globulus* aqueous extract and CuNWs obtained using different extract concentrations.

Figure 4 – FTIR spectra of *E. globulus* extract and CuNWs synthetized with distinct extract concentrations.

Figure 5 – XRD powder diffraction pattern of CuNWs synthesized with 10 mg of *E. globulus* extract compared with those of metallic copper, tenorite (CuO), cuprite (Cu_2O) and nantokite (CuCl).

Figure 6 – SEM images of CuNWs synthesized with a) 10 and b) 15 $mg.mL^{-1}$ of *E. globulus* extract.

Figure 7 – SEM images of CuNWs synthesized without the presence of oleic acid in the reactional mixture at distinct magnifications: a) 3kx and b) 10kx.

Figure 8 – TEM images of the obtained CuNWs synthesized with *E. globulus* extract: a) global view of one Cu nanowire; b) HR-TEM image obtained from the middle of a Cu wire with FFT electron diffraction image inset; c) HR-TEM image from the end of a Cu wire.

Figure 9 – XPS C 1s, Cu 2p, and Cu LMM spectra of the CuNWs with the respective peak fitting.

Figure 10 – SEM images of CuNWs obtained using standard solution of a) gallic acid and b) glucose as reducing agents.

Figure 11 – XRD patterns of a) initial CuNWs prepared with *E. globulus* extract (A) and with

glucose (B) left in b) ethanolic solution and c) normal ambient conditions. Time of air exposure:

a) 0 h and b) and c) 2 weeks.

ACCEPTED MANUSCRIPT

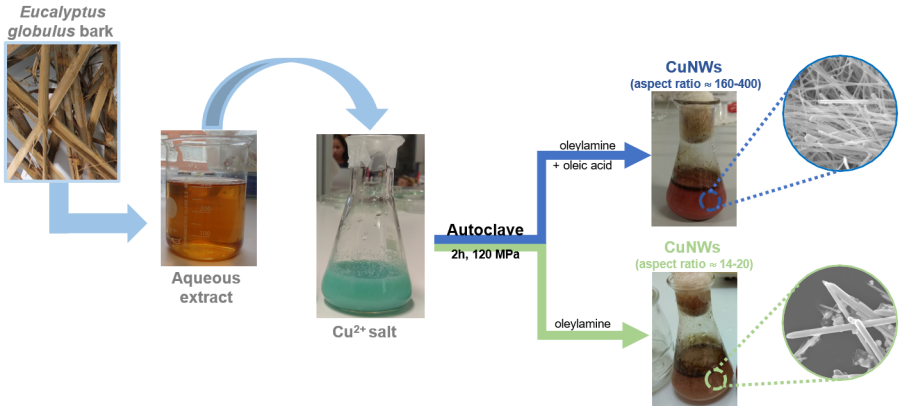

ACCEPTED MANUSCRIPT

ACCEPTED MANUSCRIPT

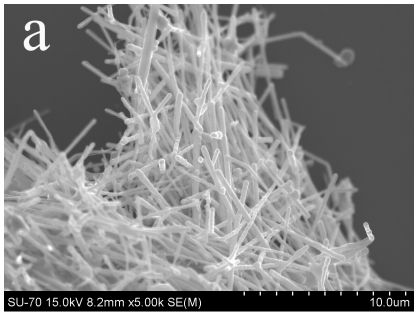

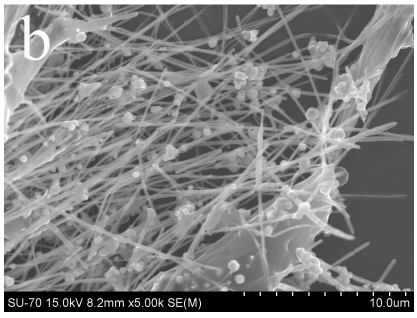

ACCEPTED MANUSCRIPT

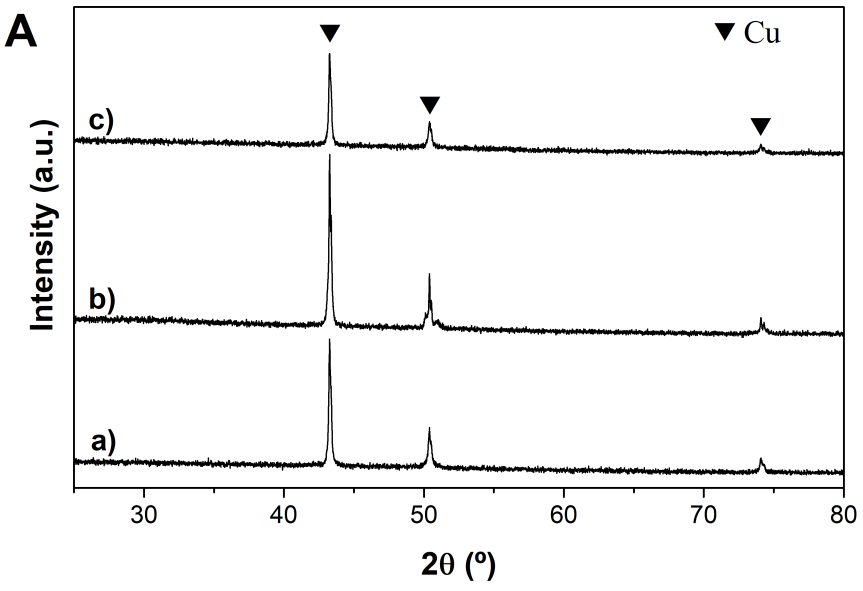

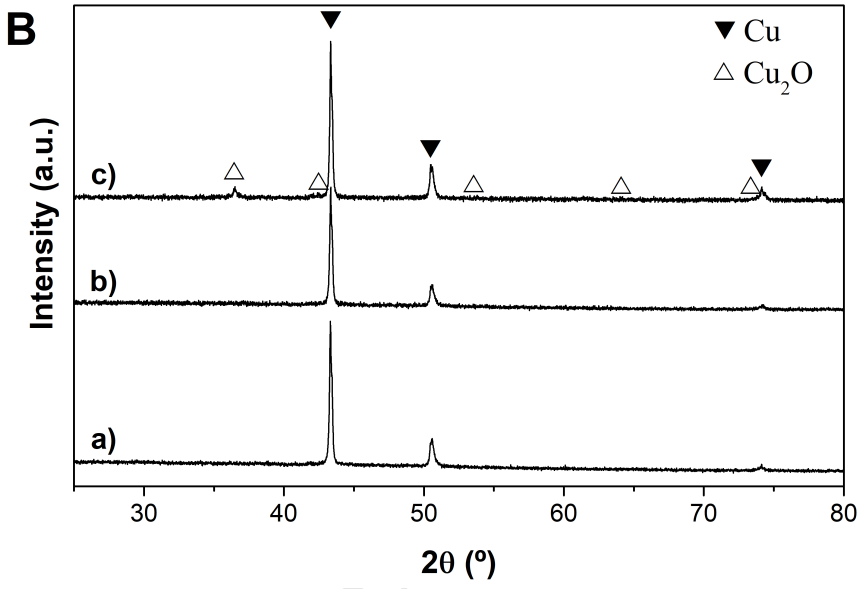

ACCEPTED MANUSCRIPT

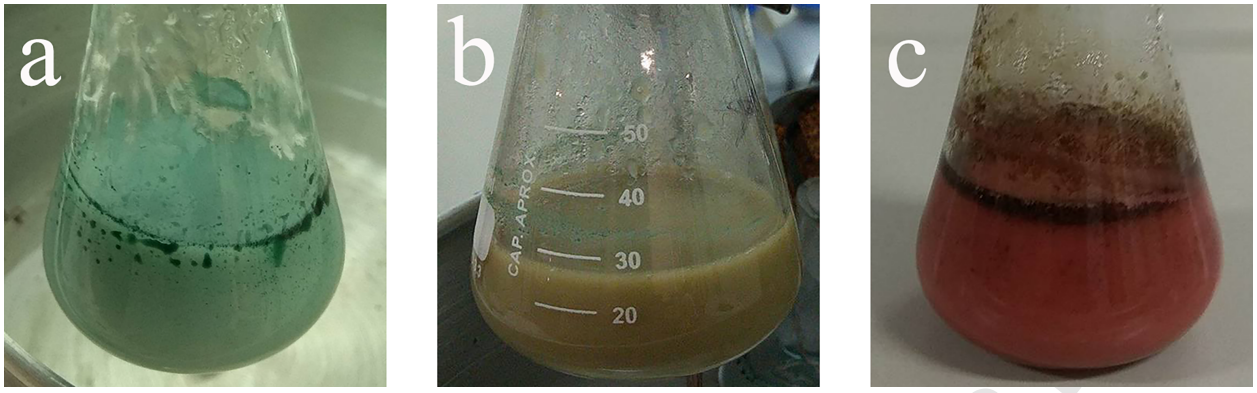

ACCEPTED MANUSCRIPT

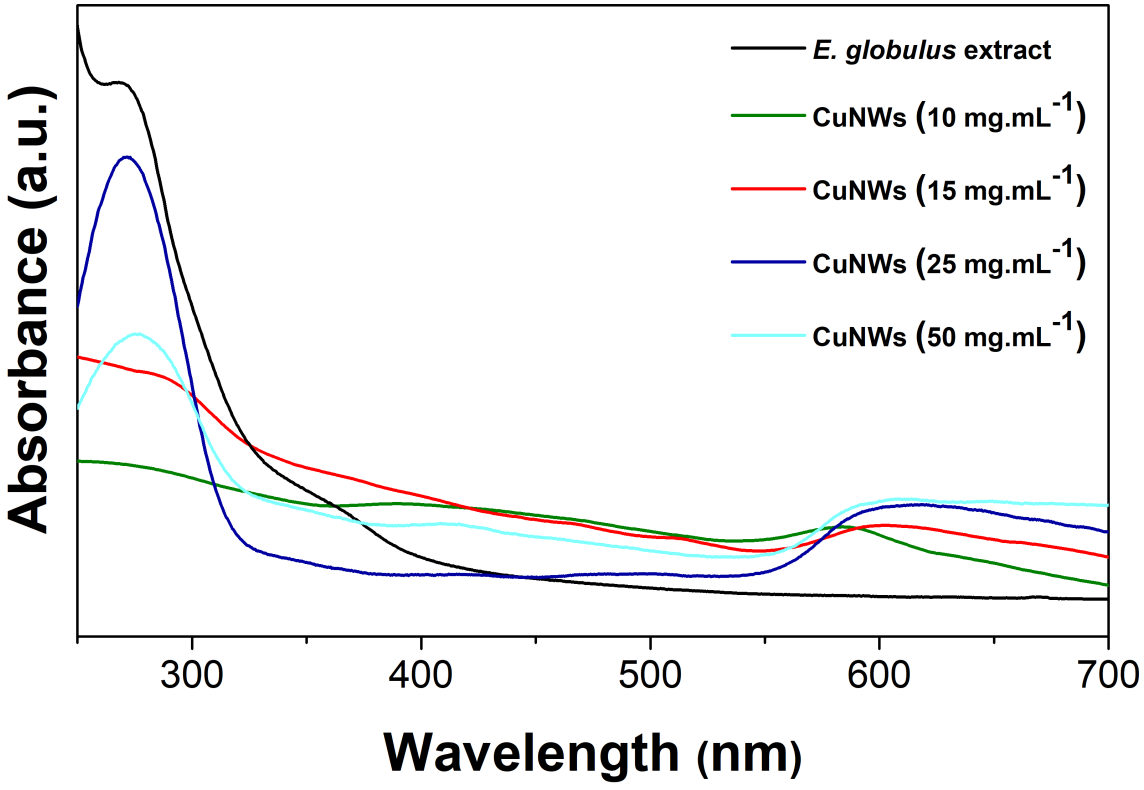
E. globulus extract
CuNWs (10 mg.mL-1)
CuNWs (15 mg.mL-1)
CuNWs (25 mg.mL-1)
CuNWs (50 mg.mL-1)
Absorbance (a.u.)
300
400
500
600
700
Wavelength (nm)

ACCEPTED

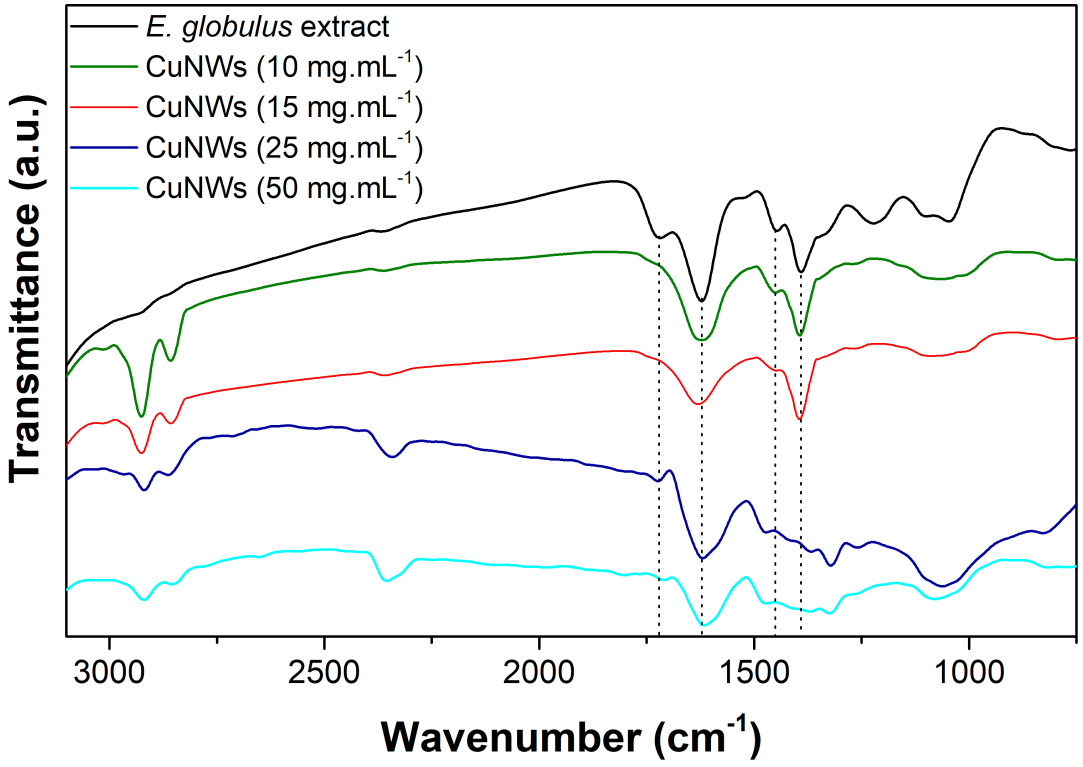
E. globulus extract
CuNWs (10 mg.mL-1)
CuNWs (15 mg.mL-1)
CuNWs (25 mg.mL-1)
CuNWs (50 mg.mL-1)
Transmittance (a.u.)
3000
2500
2000
1500
1000
Wavenumber (cm-1)

ACCEPTED

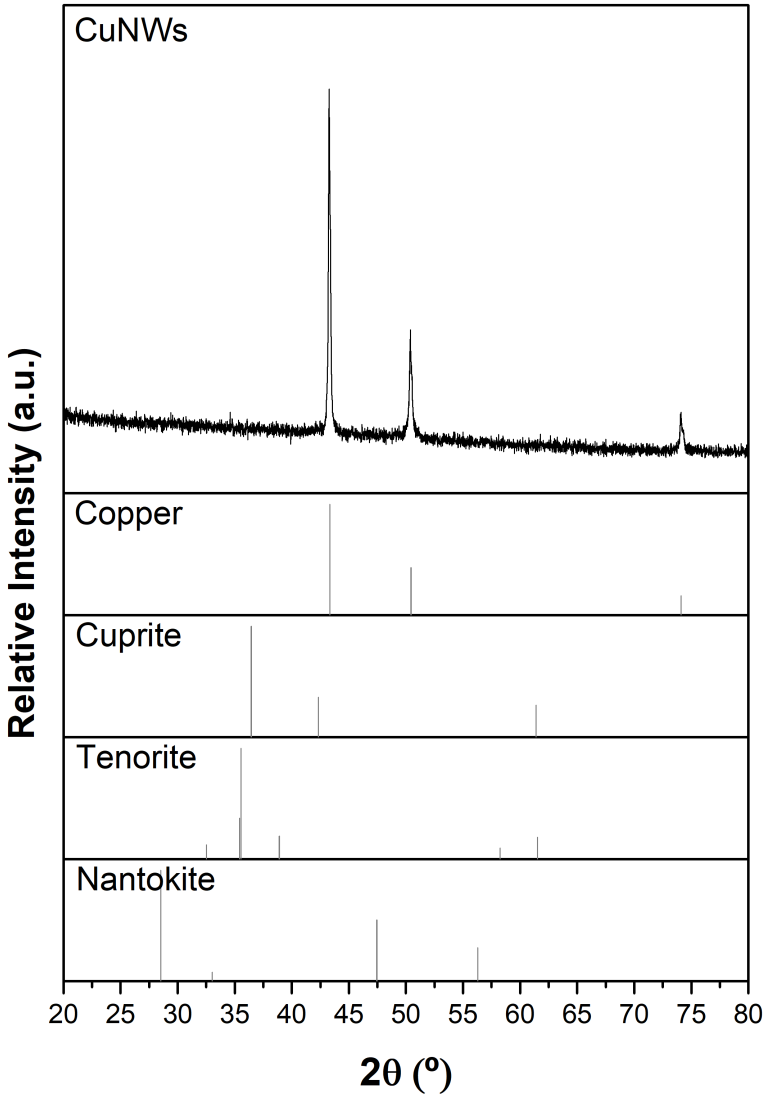

ACCEPTED MANUSCRIPT

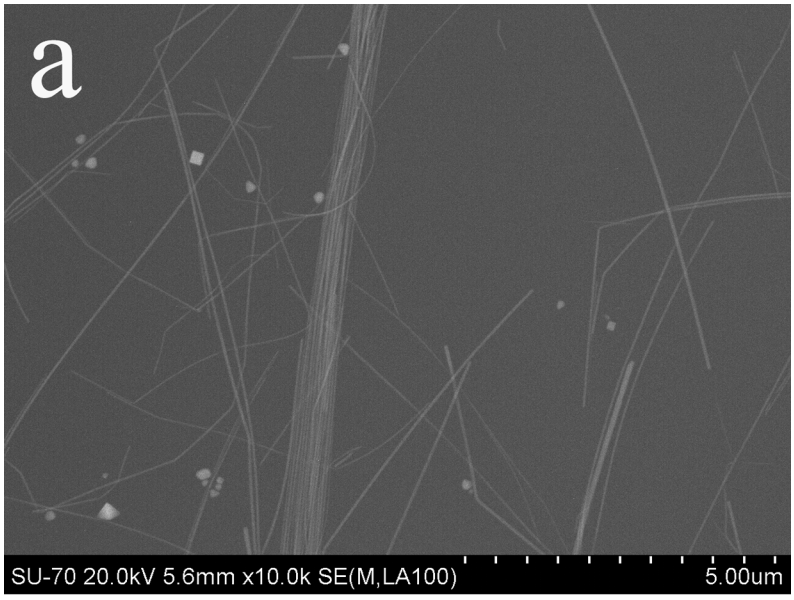

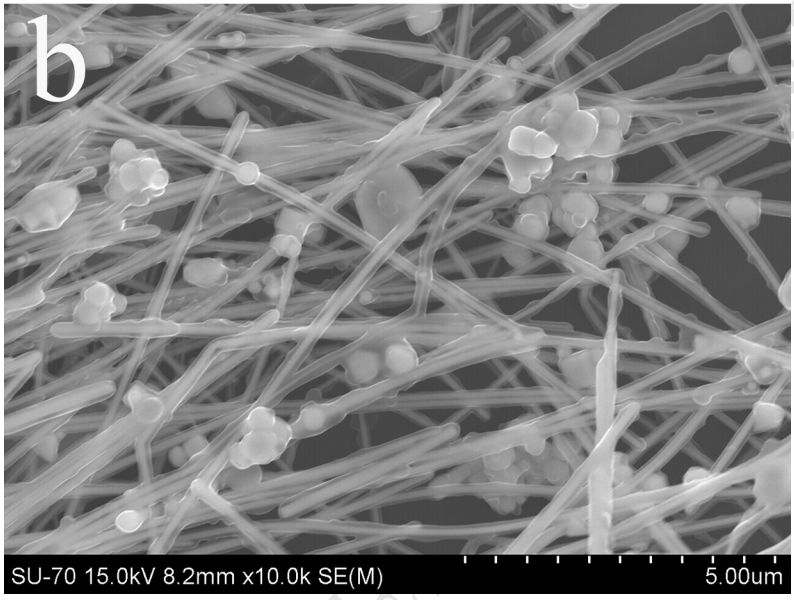

ACCEPTED MANUSCRIPT

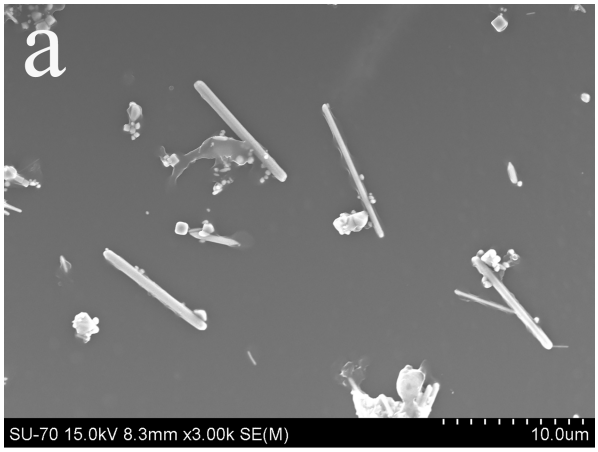

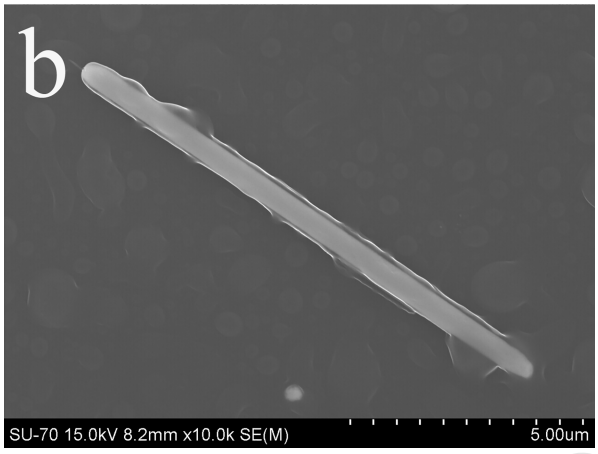

ACCEPTED MANUSCRIPT

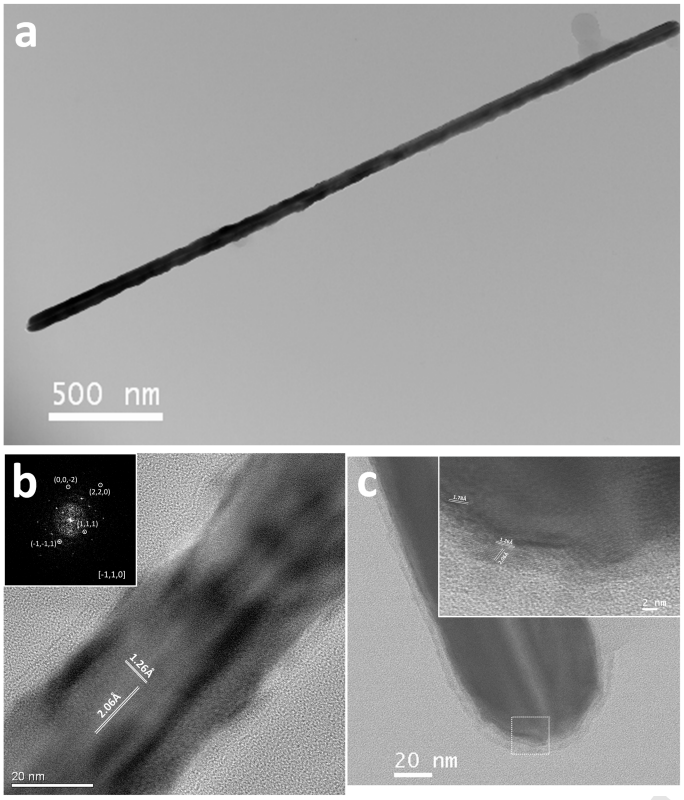

ACCEPTED MANUSCRIPT

ACCEPTED MANUSCRIPT

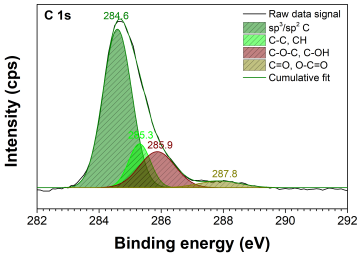

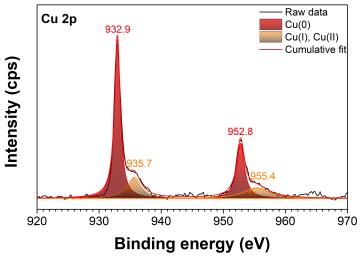

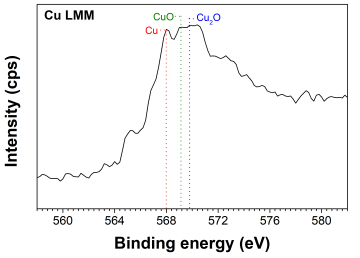

ACCEPTED MANUSCRIPT

ACCEPTED MANUSCRIPT

Highlights

• Novel and sustainable pathway to prepare copper nanowires using *Eucalyptus globulus* bark extract.

• Biosynthesized copper nanowires were confirmed by UV-vis, FTIR, XRD, SEM and TEM techniques.

• Copper nanowires biosynthesis with distinct aspect ratio can be obtained.

• Using this aqueous green approach, the use polyvinylpyrrolidone is completely unnecessary.

• Copper nanowires showed a remarkable resistance to air oxidation.

ACCEPTED MANUSCRIPT